



# Applications and challenges of thermoplasmonics

Guillaume Baffou<sup>1</sup>  , Frank Cichos<sup>2</sup>   and Romain Quidant<sup>3,4,5</sup>  

**Over the past two decades, there has been a growing interest in the use of plasmonic nanoparticles as sources of heat remotely controlled by light, giving rise to the field of thermoplasmonics. The ability to release heat on the nanoscale has already impacted a broad range of research activities, from biomedicine to imaging and catalysis. Thermoplasmonics is now entering an important phase: some applications have engaged in an industrial stage, while others, originally full of promise, experience some difficulty in reaching their potential. Meanwhile, innovative fundamental areas of research are being developed. In this Review, we scrutinize the current research landscape in thermoplasmonics, with a specific focus on its applications and main challenges in many different fields of science, including nanomedicine, cell biology, photothermal and hot-electron chemistry, solar light harvesting, soft matter and nanofluidics.**

In the 1990s, plasmonics emerged as an uprising field of research with a community mainly interested in the gigantic light intensity enhancement observed in the vicinity of metal nanoparticles under illumination at their plasmonic resonance, envisioning applications to biosensing, photovoltaics or plasmon-enhanced spectroscopy. For these photonic applications, losses in the metal and the associated heat generation were considered as side effects that had to be minimized.

In 1999, a seminal work exploited the heat generated by gold nanoparticles to induce and study the denaturation of proteins<sup>1</sup>. The authors realized for the first time the main benefits of using metal nanoparticles compared with more commonly used dyes: owing to the enhanced light-matter interaction at their plasmonic resonance, very-high-temperature increments, localized in space and time, can be created upon moderate light intensity, without thermobleaching or photobleaching the absorbers. However, this visionary work did not receive the attention it merited. The two main articles that triggered the interest of the scientific community in nanoplasmonic heating were published a few years later. The first one, published in 2002, introduced the idea of plasmonic photothermal imaging<sup>2</sup>. By combining modulated heating of individual nanoparticles with a lock-in detection, researchers were able to detect their position with very high accuracy, and use them in cell biology as labelling agents that do not suffer from photobleaching. Although this work helped the community think differently about the relevance of thermal effects in plasmonics, this technique is not widely used today. The second pioneering work proposed in 2003 was devoted to plasmonic photothermal therapy (PPTT) of cancer, relying on the internalization of gold nanoparticles in tumours to induce targeted hyperthermia under illumination<sup>3,4</sup>. The simplicity of the idea along with first encouraging preclinical results rapidly made this concept very appealing. Following these inspiring applications, several other developments based on plasmonic heating were imagined around the same time, such as drug and gene delivery<sup>5</sup> and photoacoustic imaging<sup>6</sup>. All these initial developments and many other following applications relying on the use of plasmonic nanoparticles as nano-sources of heat define the field of thermoplasmonics<sup>7–10</sup>.

Remarkably, the scope of thermoplasmonics has recently extended beyond this set of direct applications. In nanoplasmonic

systems, sample heating, unavoidable in some cases, has to be quantified to confidently determine the origin of the experimental observations, even if it is not the primary mechanism of interest. This general concern makes thermoplasmonics ubiquitous in plasmonics and more generally in nano-optics. Yet, even for those who are aware and interested in these photothermal effects, they may be difficult to apprehend, especially at the nanoscale and for the optics community, which is more familiar with propagation, interference and diffraction processes, rather than diffusion laws. Over the past decade, some debates have emerged regarding the proper way to account for photothermal processes in plasmonics, questioning the validity of some experimental observations. Today, the community is still at a stage where the influence of nanoscale photothermal processes is not fully understood and consensual.

This Review is intended to give a global and critical picture of the current research landscape in thermoplasmonics with a focus on applications. We describe the current state of the art in the most active and promising activities, from biomedicine, biology and chemistry, to solar harvesting and optofluidics, and discuss their impact, open questions and challenges. The fundamental physics governing the conversion of electromagnetic energy into heat by plasmonic nanoparticles is well covered by recent literature<sup>7–10</sup>. We, however, stress some important basics involved when bringing plasmonic heating into application within thematic boxes throughout the text.

## Hyperthermia therapy

In medicine, hyperthermia therapy uses heat to treat or complement the treatment of a disease or pathology. Depending on the applied temperature ( $T$ ) increase, heat triggers different biological and physiological mechanisms: from the stimulation of the immune system and the increment of diffusion through the cell membrane ( $T < 41$  °C), and partial cell damage and increment of blood flow ( $41$  °C  $< T < 43$  °C) to irreversible cell damage and protein unfolding ( $43$  °C  $< T < 50$  °C) and finally denaturation of proteins and DNA damage ( $T > 50$  °C.) Over the years, different sources of heat have been considered (electrical, microwave, focused ultrasounds and so on) but one had to wait until the 1960s, after the invention of the laser, to see photothermal therapy emerge, an approach that exploits natural light absorption of tissues. In this context,

<sup>1</sup>Institut Fresnel, CNRS, Aix Marseille University, Ecole Centrale Marseille, Marseille, France. <sup>2</sup>Molecular Nanophotonics Group, Peter Debye Institute for Soft Matter Physics, Universität Leipzig, Leipzig, Germany. <sup>3</sup>ICFO — Institut de Ciències Fotòniques, The Barcelona Institute of Science and Technology, Barcelona, Spain. <sup>4</sup>ICREA — Institució Catalana de Recerca i Estudis Avançats, Barcelona, Spain. <sup>5</sup>Nanophotonic Systems Laboratory, Department of Mechanical and Process Engineering, ETH Zurich, Zurich, Switzerland. <sup>✉</sup>e-mail: [guillaume.baffou@fresnel.fr](mailto:guillaume.baffou@fresnel.fr); [cichos@physik.uni-leipzig.de](mailto:cichos@physik.uni-leipzig.de); [rquidant@ethz.ch](mailto:rquidant@ethz.ch)

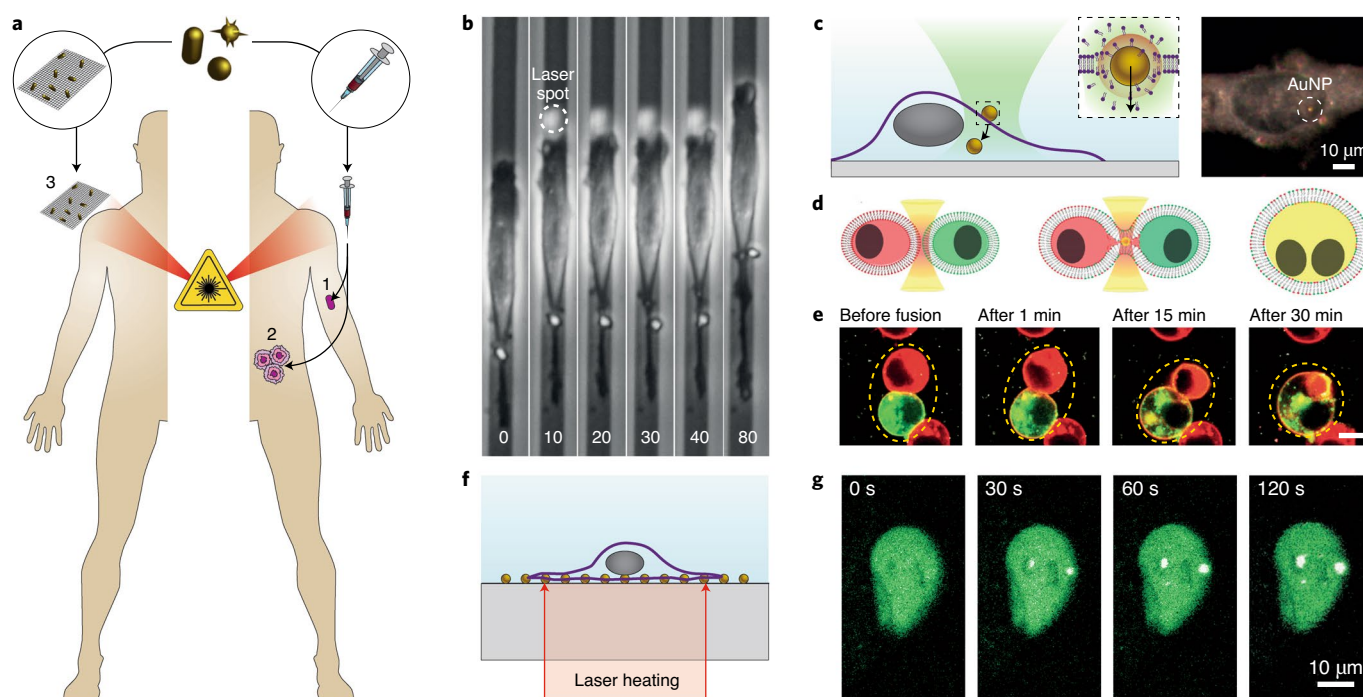


**Fig. 1 | Thermoplasmonics for photothermal therapy and cell biology.** **a**, Local delivery of plasmonic nanoparticles can be performed (1) by systemically injecting them in the blood flow, (2) through in situ injection directly in the organ/region to be treated or (3) by anchoring them at the surface of a solid support, for instance, the surface of a surgical implant. Independent of the administration mode, NIR light is then used to illuminate the accumulated nanoparticles at their plasmon resonance, to create a local increase in temperature capable of inducing local cell/bacteria death. **b**, Time lapse of a living cell migrating along a stripe of gold nanoparticles, at times 0, 10, 20, 30, 40 and 80 min. From the second to the fifth image, a laser spot has been focused in front of the cell, heating the medium, which stopped the migration. **c**, Injection of an optically trapped, heated gold nanoparticle (AuNP) through the membrane (purple line) of a living cell. **d,e**, Schematic of the principle of photothermally assisted fusion of living cells using an optically trapped gold nanoparticle (**d**) and fluorescence images of two cells being optically trapped and fused by nanoparticle heating (**e**). **f,g**, Schematic of a living cell lying on a layer of gold nanoparticles heated by laser illumination (**f**) and time lapse of a single living cell using fluorescence microscopy (**g**), where fluorescent granules are appearing, as a sign of the heat shock response. Panels reproduced with permission from: **b**, ref. <sup>35</sup>, American Chemical Society; **c**, ref. <sup>37</sup>, American Chemical Society; **d,e**, ref. <sup>38</sup>, Springer Nature Ltd; **f,g**, ref. <sup>30</sup>, Wiley.

thermoplasmonics can artificially boost light-to-heat conversion in the near-infrared (NIR) region of the spectrum where tissues are more transparent (Fig. 1a).

**Cancer therapy.** The application of PPTT to cancer treatment was first proposed in 2003, almost simultaneously by two teams<sup>3,4</sup>. The approach relies on specifically delivering plasmonic nanoparticles to cancer tissue, and using a subsequent light exposure to induce a local increase in temperature, sufficient to engender cancer cell death, while not substantially affecting surrounding healthy tissue. Since the original proposal, a multitude of plasmonic nanoparticles have been suggested as efficient photothermal agents, spanning a variety of constitutive materials, sizes and geometries<sup>11</sup>. There are several criteria to be considered when identifying the optimal plasmonic nanoparticles for PPTT: optimizing light-to-heat conversion (Box 1) in the NIR region of the spectrum where tissues feature minimum optical absorption, reducing toxicity by minimizing the total amount of metal<sup>12</sup>, and maximizing cell internalization by properly selecting the nanoparticle size and surface chemistry<sup>12</sup>.

Almost two decades of research in PPTT has led to great advances. After some first clinical trials for head and neck cancer that were not so conclusive<sup>13</sup>, promising results on prostate cancer have recently been reported, both in large animals<sup>14</sup> and patients. However, several major limitations remain to be addressed. (1) Low targeting specificity: despite extensive effort to biofunctionalize the nanoparticle surface, specific targeting is often hindered by the protein corona effect that tends to annihilate the specificity of

antibodies and other ligands<sup>15</sup>. (2) Low targeting yield: as a direct consequence of the protein corona effect, the main delivery mechanism, known as the enhanced permeability and retention effect, relies on the higher permeability of cancer tissue. As this process is rather inefficient, only about 1% of the injected nanoparticles reach the tumour<sup>11</sup>. Furthermore, the enhanced permeability and retention effect is not as systematic in humans as in animal models, leading to high variability between patients<sup>16</sup>. (3) Metal nanoparticle clearance: systemic injection of plasmonic nanoparticles in the bloodstream leads to an accumulation in filtering organs, especially in the liver and spleen. While several studies have explored potential toxicity and clearance pathways<sup>17</sup>, no clear consensus has yet been reached. (4) Difficult temperature control: in the biological environment, nanoparticles tend to agglomerate, which changes their optical properties (resonance shift and broadening). Together with the size and shape distribution of the particles and inhomogeneous cell and tissue uptake, this may cause some non-uniformity of heat delivery, and a difficulty in ensuring a uniform and controlled temperature distribution<sup>18</sup>.

Despite considerable progress, much remains to be understood about the fundamentals of PPTT in oncology, in particular on the induced cancer cell death mechanisms as well as the biological and physiological mechanisms they trigger. Also, most studies so far have reported effective results on mice with subcutaneous cancer models. However, these models are often not biomedically relevant. There is a need for more elaborated orthotopic models, based on human tumours grown on the same animal organ, which account

## Box 1 | Identifying the right thermoplasmonic nanoparticles

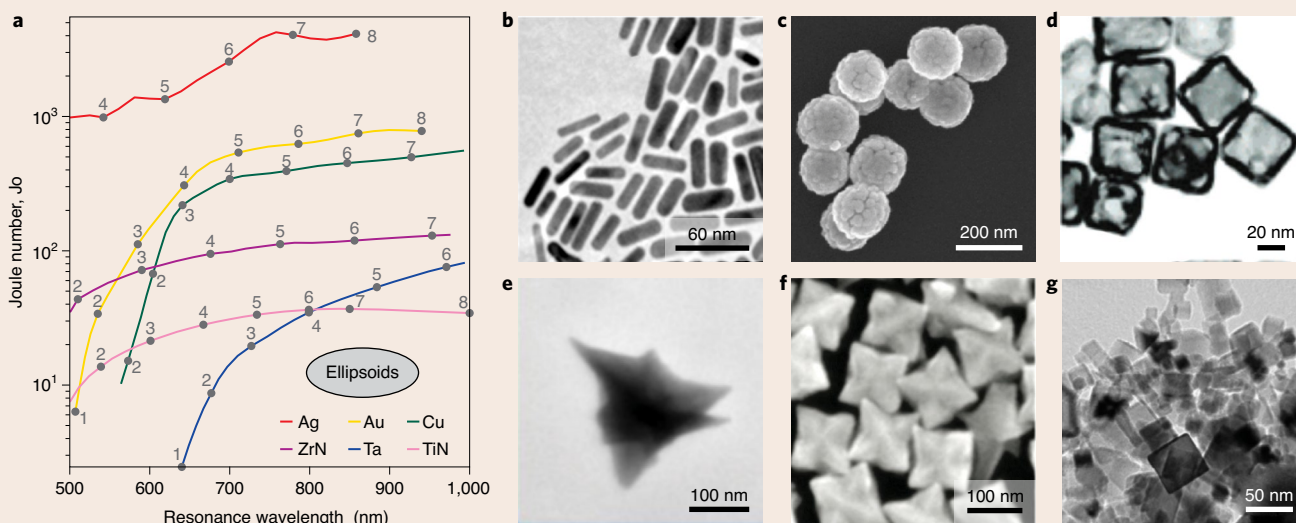
Finding the most suitable thermoplasmonic nanoparticle for a specific application is not a trivial task as it often requires compliance with several constraints that can be physical, chemical or biological in nature. To meet these constraints, one has three parameters to adjust: the nanoparticle size, its shape and composition.

A common goal for all applications of thermoplasmonics is to maximize light-to-heat conversion of the nanoparticles. This can be first achieved by increasing the size of the nanoparticles. The absorption cross-section  $\sigma_{\text{abs}}$  scales indeed as the volume ( $V$ ) of the nanoparticle, at least for small nanoparticles in the quasistatic regime (for instance, for gold nanospheres typically smaller than 60 nm). Normalizing  $\sigma_{\text{abs}}$  by the nanoparticle volume leads to a refined figure of merit that isolates the effect of shape and composition, as it no longer depends on the nanoparticle size (at least for small nanoparticles). For this reason, the Joule number has been defined as<sup>130</sup>,  $Jo = \frac{\sigma_{\text{abs}} \lambda_{\text{ref}}}{2\pi V}$ , where  $\lambda_{\text{ref}} = 1,240$  nm is an arbitrary reference wavelength to make  $Jo$  dimensionless. Panel **a** shows values of  $Jo$  at the plasmonic resonance for nanospheroids of different aspect ratios and made of various materials. These numerical simulations show the interest of deviating from a spherical shape to strongly enhance photothermal conversion efficiency at the plasmonic resonance, and red-shifting the resonance. While, for the sake of simplicity, simulations focus here on spheroids, any deviation from a spherical shape also offers the same benefits<sup>131</sup>, for instance, rods, nanoshells, nano-urchins or nanocages (panels **b–g**). Note that at resonance, one can show that  $Jo$  scales as the inverse of the imaginary part  $\epsilon''$  of the permittivity:  $Jo \approx |\epsilon'|^{3/2} / \epsilon''$  (ref. <sup>130</sup>), while

the heat power density (power per unit volume) in the material is known to scale, in contrast, as  $\epsilon''|E|^2$ . This apparent contradiction originates from the fact that the inner electric field  $E$  in the latter expression scales as  $1/\epsilon''$ . Remarkably, such a rationale explains why noble metals are more efficient plasmonic materials (see panel **a**) and remain, after two decades, the preferred plasmonic materials for both optical and thermal experiments.

The optimization of light-to-heat conversion, however, has to compromise with other requirements and hence not always the material with the best  $Jo$  is suitable. Biological and biomedical applications require combining sizes of a few tens of nanometres, which favour cellular uptake, with low toxicity and resonances in the NIR biological transparency window. In this context, gold nanoparticles are superior to silver, despite their lower  $Jo$ . The chemical and physical stability is also important, rendering silver in contact with water less useful due to aging effects that seriously alter the integrity of silver nanostructures<sup>132</sup>.

Applications such as catalysis and thermophotovoltaics may set other emphasis and require high structural thermal stability as temperatures of a few 100 to 1,000 °C are easily reached. Non-spherical gold nanoparticles, for example, reshape into spheres already at a temperature of 150 °C, altering their optical properties. While this problem can be overcome by transient heating (using a pulsed laser, for instance), embedding the nanoparticle within a matrix or coating it within a shell<sup>130</sup>, refractory materials (such as TiN and ZrN) can be more suitable at the cost of lower photothermal efficiencies.



**Optimizing the performance of thermoplasmonic nanoparticles.** **a**, Joule numbers calculated for ellipsoids made of different materials (light polarization along the longitudinal axis), and for different aspect ratios, from 1 to 8. **b–g**, Scanning electron micrographs of gold nanorods (**b**), silica-gold core-shell nanosphere (**c**), gold nanocages (**d**), gold nanostar (**e**), Au-Pd nanocrystals (**f**) and TiN nanoparticles (**g**). Panels adapted with permission from: **a**, ref. <sup>130</sup>, American Chemical Society; **b**, ref. <sup>133</sup>, American Chemical Society; **c**, ref. <sup>134</sup>, Dove Medical Press; **d**, ref. <sup>135</sup>, American Chemical Society; **e**, ref. <sup>136</sup>, American Chemical Society; **f**, ref. <sup>81</sup>, American Chemical Society; **g**, ref. <sup>137</sup>, RSC.

for key parameters such as tumour vascularization and damage of adjacent healthy tissues and living organs. Finally, an emerging natural trend is to combine PPTT with other therapies<sup>19</sup>, such as radiotherapy, chemotherapies and immunotherapies, to achieve a synergetic therapeutic effect with improved overall efficacy. Along this line, the same plasmonic nanoparticles used in PPTT have also been shown to be efficient and stable photosensitizers capable of

locally forming — under low-intensity illumination — reactive oxygen species for photodynamic therapy<sup>20,21</sup>.

**Beyond cancer therapy.** Plasmon-based hyperthermia has recently proven to be useful beyond oncology. For example, PPTT was tested to treat atheroma, a pathology associated with an abnormal local accumulation of material (lipids, cells, tissues and so on) in artery

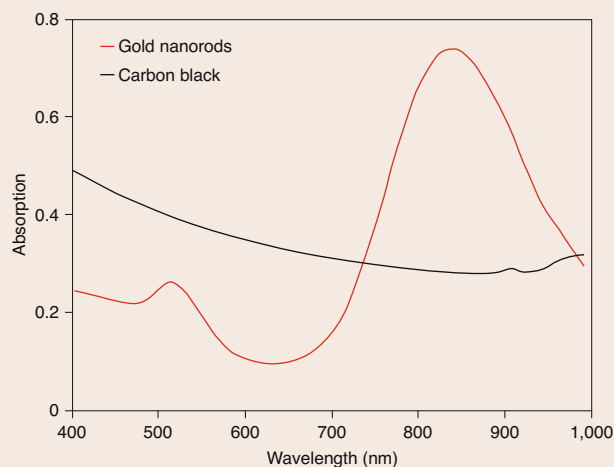
**Box 2 | Plasmonic versus non-plasmonic heating**

The main incentive for using plasmonic nanoparticles as photothermal agents is their ability to efficiently generate heat in nanoscale volumes. This asset stems from the combination of four properties of plasmonic materials: the absence of thermo-/photobleaching (unlike dyes), a high density of free electrons due to their metallic nature, low losses for noble metals (see Box 1) and the existence of resonances that enhance light–matter interaction. This unique combination makes them the best candidates for applications requiring spatially confined heating, like in nanochemistry, nanosurgery, photothermal and photoacoustic imaging. Plasmonic heating is also relevant to applications requiring temporal confinement of heat generation (for instance, in photoacoustic imaging), typically on the nanosecond scale, as the heating timescale varies as the square of the size of the heat source.

Conversely, when aiming for macroscale heating, the interest in using nanoscale absorbers is less obvious. The absorption cross-section  $\sigma_{\text{abs}}$  and the absorber size are no longer the only parameters of interest. The concentration  $c$  also becomes an important parameter one can play with to arbitrarily increase what only matters in this case: the absorbance  $A$  of the sample, defined as  $A = \sigma_{\text{abs}} c l$ , where  $c$  is the molecular concentration (in molecules per  $\text{m}^3$ ) and  $l$  is the thickness of the system. In this context, the presence of plasmonic resonances is not necessary to achieve near 100% absorption. Other materials, such as chromium (used for microscale thermophoresis studies<sup>102</sup>) or even black paint or carbon black, could be used as well. The latter can easily achieve, by increasing  $c$ , near-100% absorption at low cost. Moreover, these black materials feature a high absorbance over a much larger spectrum than what resonant nanoparticles can offer (see the figure), which becomes advantageous when involving broadband illumination, for instance, for solar-light-based applications.

This reasoning does not mean that the use of plasmonic nanoparticles for macroscale heating is never relevant, and can

be always replaced by cheaper black materials. For instance, macroscale plasmonic heating offers a real interest when the absorbance has to be confined over a restricted wavelength range (see the figure), for instance, to ease fluorescence imaging in cell biology (see ‘Cell biology’) or for white and colourful three-dimensional printing (see ‘Additive manufacturing’). Using gold nanoparticles also offers advantages when delivered to living organisms for hyperthermia applications, because of their friendly biofunctionalization properties and biocompatibility. However, for applications involving broadband solar absorption, the interest of using plasmonic nanoparticles over carbon black is not evident.



**Absorption spectra of 0.01 g l<sup>-1</sup> solutions of carbon black and silica-coated gold nanorods (12.5 nm × 50 nm), suspended in ethanol.** Reproduced with permission from ref. <sup>129</sup>, American Chemical Society.

walls, leading to a restriction of blood flow, increasing the risk of a heart attack. In 2015, successful phase II clinical trials were carried out, demonstrating a substantial regression of atheroma by PPTT<sup>22</sup>. Atheroma therapy does not suffer from some of the limiting constraints of cancer therapy. In particular, unlike for cancerous tumours, eliminating the whole atheroma is not a stringent requirement as partial elimination is already beneficial as soon as it improves the blood flow. Note that similar emerging therapies using PPTT, such as the treatment of retinal degenerative disease<sup>23</sup>, hair removal<sup>24</sup> and acne treatment<sup>25</sup>, have also been proposed.

**Sterilization and disinfection.** Similar to cells, most bacteria viability is altered when experiencing a temperature greater than 45 °C. One can thus follow a similar PPTT strategy for applications to sterilization and disinfection. In 2006, a method to selectively kill bacteria *in vitro*, based on targeting their wall with bioconjugated gold nanoparticles before shining them with nanosecond-pulsed laser light, was proposed<sup>26</sup>. This concept is particularly relevant to the field of disinfection of surgical implants. Implant contamination has indeed become a major health issue, especially when bacterial colonization ends up forming a biofilm making them even more resistant to antibiotic treatment. A first proof of principle showing the use of PPTT to treat biofilm *in vitro* was reported in 2017<sup>27</sup> and this concept has recently been extended to surgical implants<sup>28</sup>. In this last study, to avoid the issues related to systemic injection of nanoparticles, such as the unspecific nanoparticle delivery and clearance, the authors proposed to have them directly anchored at the surface of the implant, a polymer mesh used in hernia repair,

which was chemically modified to host a high-density monolayer of gold nanorods (Fig. 1a). PPTT treatment, in the form of a train of broadband light pulses, showed clinically relevant biofilm degradation, associated with the alteration of the biofilm superstructure.

Sterilization of medical instruments using a thermoplasmonic approach was proposed in 2013<sup>29</sup>. In this proof-of-principle experiment, solar radiation was focused on a high-concentration aqueous solution of gold nanoshells. The formed water steam was extracted through a nozzle and sent to a sterilization module. The authors reached a sterility level compatible with the Food and Drug Administration regulation. While plasmonic nanoparticles as absorption agents are advantageous in biomedicine, because they allow the generation of local heating through tissue using NIR illumination, their benefit over black absorbers made of dyes or carbon black is not always obvious for other applications involving broadband illumination, such as solar light, as discussed in Box 2.

**Cell biology**

More fundamentally, all building blocks of living cells are highly temperature responsive: lipid layers can undergo phase transitions, proteins can unfold, DNA can melt and so on. Investigating all these effects *in vitro* demands a precise control of the temperature of the sample, which is normally achieved by combining resistive macroscopic heating and thermocouple measurements. Selective laser heating of biological *in vitro* samples has been proposed as a powerful alternative approach. Along with the use of plasmonic nanoparticles as efficient light absorbers, this approach offers three major benefits compared with resistive macroscopic heating. (1) Reduced

spatial scale: coupling the heating laser to an optical microscope enables heating over a micrometric area, offering the possibility, for instance, to heat a single living cell while leaving the other adjacent cells unaffected for subsequent measurements<sup>30</sup>. In this way, a range of temperature conditions can be applied within a single multiwell plate or Petri dish. One can even heat subcellular compartments or single organelles, leading to the possibility to answer fundamental questions in thermal biology. (2) Reduced timescale: experiments at the microscale imply that the targeted temperature increase is achieved within around 1 ms, giving a well-defined time zero to study the dynamical response of a biological system, which can be faster than a second. In contrast, macroscopic heating with resistive heating usually involves timescales on the order of several minutes, or several seconds at best. (3) Large achievable temperature: high local temperature increases under pulsed illumination can find application in nanosurgery or optoporation, as detailed in the next paragraph. Even under continuous-wave illumination, one can achieve high temperatures, unreachable using conventional macroscopic heating without damaging the microscope or the objective lens, or affecting the immersion oil or the setup alignment<sup>31</sup>.

As mentioned above, the benefits of using gold nanoparticles with laser heating in biology was already recognized in 1999<sup>1</sup>. Laser heating of gold nanoparticles enabled the researchers at that time to study the denaturation of chymotrypsin proteins up to 470 K, in the context of the photothermal treatment of pigmented cells. A decade later, experiments focused on a variety of other biomolecules *in vitro*, such as lipid layers<sup>32</sup> (artificial flat membranes, giant unilamellar vesicles), DNA<sup>33</sup>, proteins and amyloid fibrils<sup>34</sup>. Furthermore, more sophisticated experiments have been conducted in living cells, bacteria and eukaryotic cells, for fundamental research, for example, for controlling cell migration<sup>35</sup> (Fig. 1b), cell optoporation<sup>36</sup> and transfection<sup>37</sup> (Fig. 1c), cell fusion<sup>38</sup> (Fig. 1d,e) and heat-shock response<sup>30</sup> (Fig. 1f,g), and for applications, such as nanosurgery<sup>39</sup>. Plasmon heating can also be used to locally release molecules within cells<sup>40</sup>: biomolecules, drugs and genes can be directly loaded at the surface of a plasmonic cargo or encapsulated in micelles, liposomes or even red blood cells, decorated with plasmonic nanoparticles<sup>40–42</sup>. Upon illumination, the local temperature increase induces a molecular release via either bond breakage or phase change. These approaches, however, require heating to remain below a few kelvin to avoid affecting cellular metabolism. Remarkably, a similar approach can also be applied to release cells anchored to a plasmonic substrate<sup>43</sup>.

All these studies represent the onset of a fast-growing field of research that could be named ‘single-cell thermal biology’, and where thermoplasmonics is expected to have a major role.

### Photothermal and hot-electron chemistry

Temperature is a common parameter to control chemical transformations. According to the Arrhenius law, the rate constant  $K$  of a chemical reaction and its molar activation energy  $E_a$  are related via an exponential law:  $K \propto \exp(-E_a/RT)$ , where  $T$  is the temperature and  $R$  is the gas constant. Plasmonic nanoparticles can be used to boost chemical reactions based on such a local temperature variation but also with optical near-field enhancement and hot-carrier injection<sup>44</sup>. This paradigm represents an important research area in plasmonics with pivotal, societal and economic impact as it could contribute to cleaner energies<sup>45</sup>. In particular, hot-electron injection involves metal electrons of a few electronvolts capable of driving reactions that could not occur otherwise via conventional heating. But in this approach, even if optical heating is not the process of interest, it has to be carefully considered to ensure the validity of the underlying catalytic mechanism. For these reasons, the rest of the section will be divided into two parts: in the first part, plasmonic heating is the targeted process to assist chemical reactions<sup>46</sup>; whereas the second part is oriented towards hot-carrier plasmonics<sup>45</sup>.

**Photothermal chemistry.** The use of thermoplasmonics in chemistry raises an important question: what are the specific benefits of using light-induced plasmonic heating, over regular heating with a hot plate? First, thermoplasmonics offers a spatial confinement that enables micro-/nanopatterning of the chemical products on a surface<sup>47</sup>. Second, plasmonic heating can yield a high temperature increase under moderate illumination intensity up to a superheated state of the solvent. Upon pulsed illumination, the temperature increase is so brief and confined around each nanoparticle that no macroscopic boiling is observed even at nanoparticle temperatures close to 300 °C, the spinodal temperature of water<sup>48</sup>. Even continuous-wave illumination can yield a superheated state of water as high as 220 °C (ref. <sup>31</sup>). In the case of a plasmonic substrate in contact with a gas phase (no liquid), the temperature of the illuminated area can be locally increased by several hundreds of degrees, while the chamber itself remains at moderate temperature, making the experimental conditions less stringent and the reaction less energy consuming<sup>47</sup>. A third advantage of plasmonic nanoparticles is that they can also feature catalytic activity, especially when sized down to a few nanometres<sup>49</sup>.

Applications in photothermal chemistry can be divided in three categories: (1) plasmonic-assisted chemical vapour deposition (PACVD) in a vacuum chamber, (2) thermoplasmonic-assisted catalysis in the gas phase and (3) thermoplasmonic-assisted enhanced reactivity in solution. Chemical vapour deposition (CVD) is a thin-film deposition technique on a substrate at high temperature, under vacuum, from volatile molecules that react and adsorb on the substrate. As an alternative to homogeneous resistive heating, it was proposed to locally heat the substrate with light to spatially control the growth. PACVD was first reported in 2006 and demonstrated the micropatterning of TiO<sub>2</sub> and PbO on glass (Fig. 2a,b)<sup>50</sup>. Nanoscale subdiffraction PACVD can also be achieved when single nanoparticles are heated, as corroborated in 2007 with the growth of silicon, germanium or carbon nanowires (Fig. 2c,d)<sup>47</sup>. In the gas phase, the association of gold nanoparticles and metal oxides such as titania (TiO<sub>2</sub>) has been used since 1987 to yield a substantial catalytic activity even at moderate temperature increase<sup>49</sup>. In 2008, it was proposed to heat such a system with light instead of with a hot plate, benefiting from the strong plasmonic absorption of the gold nanoparticles themselves<sup>51</sup>. In that case, heating was limited to the catalytically active area, reducing the overall energy consumption. In 2010, the benefit of laser heating over global resistive heating was demonstrated to yield a gain of two to three orders of magnitude<sup>52</sup>.

This approach has been extended to the liquid phase since 2009 (Fig. 2e,f)<sup>53</sup>. Different strategies have been used to achieve high temperatures that cannot be normally reached in water without boiling, for instance, using a nanosecond-pulsed laser<sup>54</sup> and using a continuous-wave laser on a glass substrate. This second approach can yield temperatures as high as 200 °C without boiling the fluid, opening the path for hydrothermal chemistry at ambient pressure, avoiding the use of an autoclave and a closed reaction medium (Fig. 2g,h)<sup>31,55</sup>.

**Plasmonic hot-carrier chemistry.** The absorption of a photon by a metal nanoparticle promotes one electron from the conduction band by an energy that equals the photon energy, that is, of the order of a few electronvolts in the visible–NIR range. The associated electron and hole created this way are known as ballistic hot carriers. While these hot carriers only live for tens of femtoseconds due to collisions with the other unexcited electrons of the particle<sup>48</sup>, they can, during their short lifetime, interact with surrounding molecules to drive chemical reactions<sup>45</sup>. In particular, they can be transferred to adsorbed molecules to induce redox processes. Along with this indirect charge transfer mechanism, a direct charge transfer mechanism has been proposed, where the excited

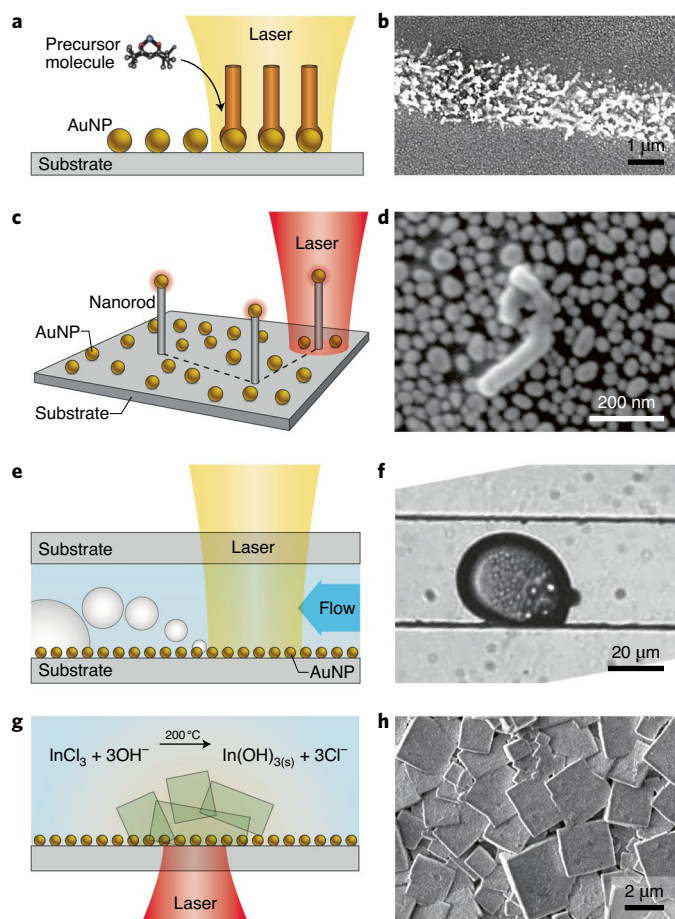


**Fig. 2 | Thermoplasmonics for chemistry.** **a,b**, PACVD. **a**, Schematic of a PACVD process showing a template of nanoscale gold dots (yellow spheres) exposed to a gaseous environment containing the CVD precursor (top left molecule). A laser illumination is locally heating the system to yield the formation of nanowires (brown). **b**, Scanning electron microscopy (SEM) image showing an example of an area of nanowires grown by PACVD. **c,d**, Subdiffraction PACVD. **c**, Schematic showing the illumination of gold nanoparticles (yellow spheres) leading to the growth of gold-catalysed nanowires along the path (dashed arrows) of the illumination beam (red beam). **d**, SEM image of the resulting isolated germanium nanowires. **e,f**, Liquid-phase plasmon assisted catalysis. **e**, Schematic of laser light heating a gold nanoparticle layer in contact with a liquid (light blue) between two substrates (grey) to form a gas bubble (white) that reacts on the nanoparticles acting as catalysts. **f**, Optical image of the formed bubble under illumination. **g,h**, Plasmon-assisted hydrothermal chemistry. **g**, Schematic showing the laser illumination of a layer of gold nanoparticles on a substrate (grey) enabling the heating of an aqueous solution at around 200 °C to allow the growth of indium(III)-hydroxide crystals (rectangles). **h**, SEM image of the resulting crystal products. Panels adapted with permission from: **a,b**, ref. <sup>50</sup>, American Chemical Society; **c,d**, ref. <sup>47</sup>, American Chemical Society; **e,f**, ref. <sup>53</sup>, American Chemical Society; **g,h**, ref. <sup>55</sup>, American Chemical Society.

hot electron directly populates a state of a molecule adsorbed on the nanoparticle surface<sup>45</sup>. Originally proposed in 2004<sup>56</sup>, the idea of plasmonic hot-carrier chemistry really attracted the interest of the community only from 2011, motivated by some seminal articles (refs. <sup>57,58</sup>, among others) that stressed the colossal envisioned industrial and societal impacts, in particular for driving chemical reactions such as water splitting<sup>58</sup> for dihydrogen production, or many redox reactions of industrial interest<sup>45</sup>. After more than a decade

of extensive activities, the field of plasmonic hot-carrier chemistry experiences heated debates regarding the actual underlying mechanisms<sup>3,59,60</sup>. In some seminal studies, the reaction rate enhancement by a hot-carrier mechanism was questioned in favour of a simple temperature increase, unexpectedly important due to the presence of collective thermal effects (see Box 3). This awareness appeared around 2018 and since then, extensive efforts have been made to address this question<sup>60</sup>. Thermoplasmonics is now playing an unforeseen but substantial role in this field of research, as it is key to better interpret experimental observations.

### Solar light harvesting

The power of plasmonic particles to convert electromagnetic energy into heat is also of potential interest in solar light harvesting. Three major fields with two different approaches arise. On the one hand, nanofluids consisting of solutions of plasmonic particles are used for volumetric heating and accordingly employed for solar energy collection and water desalination. On the other hand, thermophotovoltaics addresses the heat management in general and provides advanced concepts for solar energy conversion into electricity.

**Thermophotovoltaics.** Photovoltaics with standard p–n junctions is limited by the fact that, from the broad distribution of solar photon energies, only the bandgap energy contributes to generate electron–hole pairs. The excess energy of photons above the bandgap is converted into heat and subbandgap energy is lost completely. For this reason, the photovoltaic conversion in these simple systems is limited to around 41%, known as the Shockley–Queisser limit<sup>61</sup>. This limit can be overcome with costly multi-layer structures<sup>62</sup> with multiple bandgaps. A different and very promising approach is to get rid of thermal losses by turning all electromagnetic energy into heat<sup>63</sup>. In thermophotovoltaics, solar electromagnetic energy is first converted into heat by an efficient absorber connected to a thermal emitter releasing the heat into thermal emission with an energy close to the bandgap of a photovoltaic cell and thus converting almost all solar energy into electricity (Fig. 3a,b). Limits of solar energy conversion beyond 80% have been predicted<sup>63</sup> and efficiencies up to 29% have so far been demonstrated<sup>64</sup>. To reach theoretical efficiencies, research requires overcoming three major challenges. First, highly efficient absorbers for the solar spectrum have to be designed, which are able to convert the absorbed energy into heat. Second, the visible absorber has to be interfaced to an infrared thermal emitter that generates the thermal radiation for a photovoltaic cell with a low bandgap around 0.8–1.1 eV. This energy range requires an emitter temperature between 1,000 K and 2,000 K, which sets the strongest limitation on the choice of possible materials.

Owing to their efficient light-to-heat conversion (Box 1), plasmonic materials are a suitable class of materials for thermophotovoltaics. Yet, metals are not always able to withstand the high required temperatures (Box 1) although some studies reported efficient absorber structures of gold stable up to 1,000 K owing to a dielectric coating<sup>65</sup>. Thermally stable absorber materials are cermet, a combination of ceramics and metal particles where the metal is responsible for absorptive properties<sup>66</sup>. Cermet have been fabricated from metal particles such as nickel embedded in Al<sub>2</sub>O<sub>3</sub>. These materials yield a high absorbance of the solar range but low emittance at wavelengths above 3 μm (Fig. 3c,d)<sup>67</sup>. Refractory materials may have plasmonic properties in the visible range<sup>68</sup> but also a large imaginary part of the permittivity (W, TiN, Mo and so on), which is counter-intuitively detrimental for thermoplasmonics applications (Box 1). Well-designed metamaterial structures may be created to modify the electromagnetic density of states tailoring absorption and emission spectral shape (Fig. 3e,f)<sup>60,70</sup>. Metamaterials made of TiN (ref. <sup>71</sup>) or W–HfO<sub>2</sub> have shown to be stable up to 1,400 °C (ref. <sup>72</sup>) and photonic crystals of refractory materials have been realized

**Box 3 | Collective photothermal effects in plasmonics**

Frequently, the temperature increase in a system composed of plasmonic nanoparticles is estimated using the simple expression<sup>138</sup>:

$$\delta T = \frac{\sigma_{\text{abs}} I}{4\pi\kappa R_{\text{eq}}} \quad (1)$$

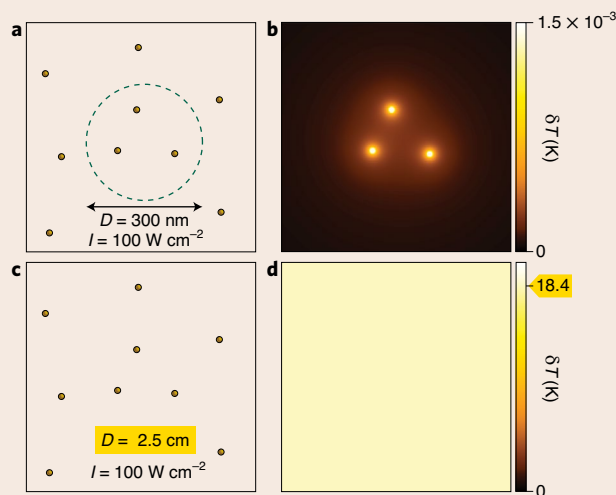
which gives the temperature increment of a single nanoparticle, of absorption cross-section  $\sigma_{\text{abs}}$ , where  $I$  is the irradiance (power per unit area) of the incoming light,  $\kappa$  is the thermal conductivity of the surrounding medium and  $R_{\text{eq}}$  is the equivalent nanoparticle radius. However, this single-nanoparticle expression can yield wrong estimations when several nanoparticles are illuminated at once, as the temperature increase experienced by a nanoparticle  $j$  also stems from the neighbouring nanoparticles  $i$  heating their environment<sup>139,140</sup>:

$$\delta T_j = \frac{\sigma_{\text{abs},j} I}{4\pi\kappa R_{\text{eq}}} + \sum_{i \neq j} \frac{\sigma_{\text{abs},i} I}{4\pi\kappa |r_i - r_j|} \quad (2)$$

Counterintuitively, the last term of equation (2) can become dominant, even for a sparse nanoparticle distribution. This effect originates from the long-range temperature diffusion profile around a source of heat, decaying as  $\delta T(r) \propto 1/r$ ,  $r$  being the distance from the heat source. The figure illustrates these so-called collective photothermal effects in a two-dimensional distribution of nanoparticles: at a constant irradiance  $I$ , varying the illuminated area from 300 nm to 2.5 cm leads to the appearance of substantial photothermal collective effects, characterized by two main features: (1) a strong overall temperature increase, several orders of magnitude higher than what equation (1) predicts and (2) a completely uniform temperature distribution, despite the nanoscale nature of the heat sources and their large separation distance.

The importance of photothermal collective effects can be estimated by calculating the dimensionless number<sup>139</sup>  $\xi = p^2/3RD$ , where  $p$  is the mean first-neighbour interdistance,  $R$  is the radius of the nanoparticle and  $D$  is the characteristic size of the

two-dimensional nanoparticle distribution under illumination. Collective effects become dominant when  $\xi < 1$ . Remarkably, not only the nanoparticle interdistance matters, but also their number (via  $D$ ), a feature proper to diffusion processes that has no counterpart in optics. In practice, neglecting these collective photothermal effects can lead to a substantial underestimation of heating and misleading interpretations of experimental data<sup>60</sup>.

**Numerical simulations illustrating collective photothermal effects**

**in plasmonics.** **a**, Schematic of the system: a uniform, not-necessarily periodic, two-dimensional nanoparticle distribution ( $R = 7$  nm,  $p = 200$  nm), illuminated with a beam of irradiance of  $100 \text{ W cm}^{-2}$  and a diameter of  $D = 300$  nm ( $\xi \approx 6$ ). **b**, Associated temperature increase showing localized hotspot, consistent with  $\xi > 1$ . **c**, Schematic showing the same system of nanoparticles as before, with a beam radius of  $D = 2.5$  cm ( $\xi \approx 10^{-4}$ ). **d**, Associated temperature increase that is fully uniform, consistent with  $\xi < 1$ .

to form thermophotovoltaic emitter structures<sup>69</sup>. An even more promising yet technologically more challenging approach is to use the near fields of the infrared emitters<sup>73</sup>. If one manufactures tiny gaps, on the order of a wavelength, between the thermal emitter and receiver, the evanescent near field of the thermal excitation can strongly contribute to the electromagnetic energy transfer by optical tunnelling<sup>73</sup>. Such near fields of surface plasmon polaritons do not follow the far-field blackbody statistics but have a high density close to the plasmon frequency<sup>74</sup> and can thus be highly spectrally selective<sup>75</sup>. While there is a growing number of promising theoretical analysis of near-field thermophotovoltaics with plasmonic structure, including graphene<sup>74,76</sup>, experimental realizations are still few<sup>77</sup> but will certainly increase in the near future.

**Nanofluids for solar energy harvesting.** Nanoparticle solutions were first coined nanofluids in 1995. Since then, there has been large interest with substantial controversy regarding their thermal properties<sup>78</sup>. Most of the recent interest in nanofluids containing various metal particles stems from their absorptive properties and their use in solar thermal energy conversion for thermal power generation, desalination of seawater or water splitting. For these applications, an absorbing material would be brought in contact with a working fluid, which is often a liquid, to transfer the heat from the absorber to the liquid. The advantage

of nanofluids is that the absorber is now directly brought into the liquid, providing a volumetric and not an interfacial heating<sup>79,80</sup>. In the case of plasmonic materials, however, the absorption spectra have to extend to larger spectral ranges by using specific structures or materials (Box 2). Suggestions of using Janus particles — polymer or silica particles with a half-sided metal coating — have been made to cover a large fraction of the solar spectral range<sup>79</sup>. Other approaches involve metal nitrides<sup>81</sup> or mixtures of different gold nanoparticle sizes<sup>82</sup> and shape<sup>83</sup>. Such immersed nano-absorbers could indeed enhance the efficiency of solar collectors<sup>79,80</sup>; however, their applications for desalination<sup>84</sup> or water splitting seem ineffective<sup>79</sup>.

**Water desalination.** About 97% of water on Earth exists in form of seawater, and freshwater availability is one of the global challenges for humanity. Cost-effective seawater desalination could therefore provide a sustainable source of fresh water for the future and sets a technological challenge. Techniques to desalinate water can be roughly split into two classes relying either on membranes (for example, for reverse osmosis) or on thermal processes<sup>85,86</sup>. Reverse osmosis plants are currently most efficient, requiring less than 3 kW h energy per cubic metre of desalinated water, a factor of three above the thermodynamic limit based on the free energy change when mixing salt and water<sup>86</sup>. Desalination based on solar-thermal

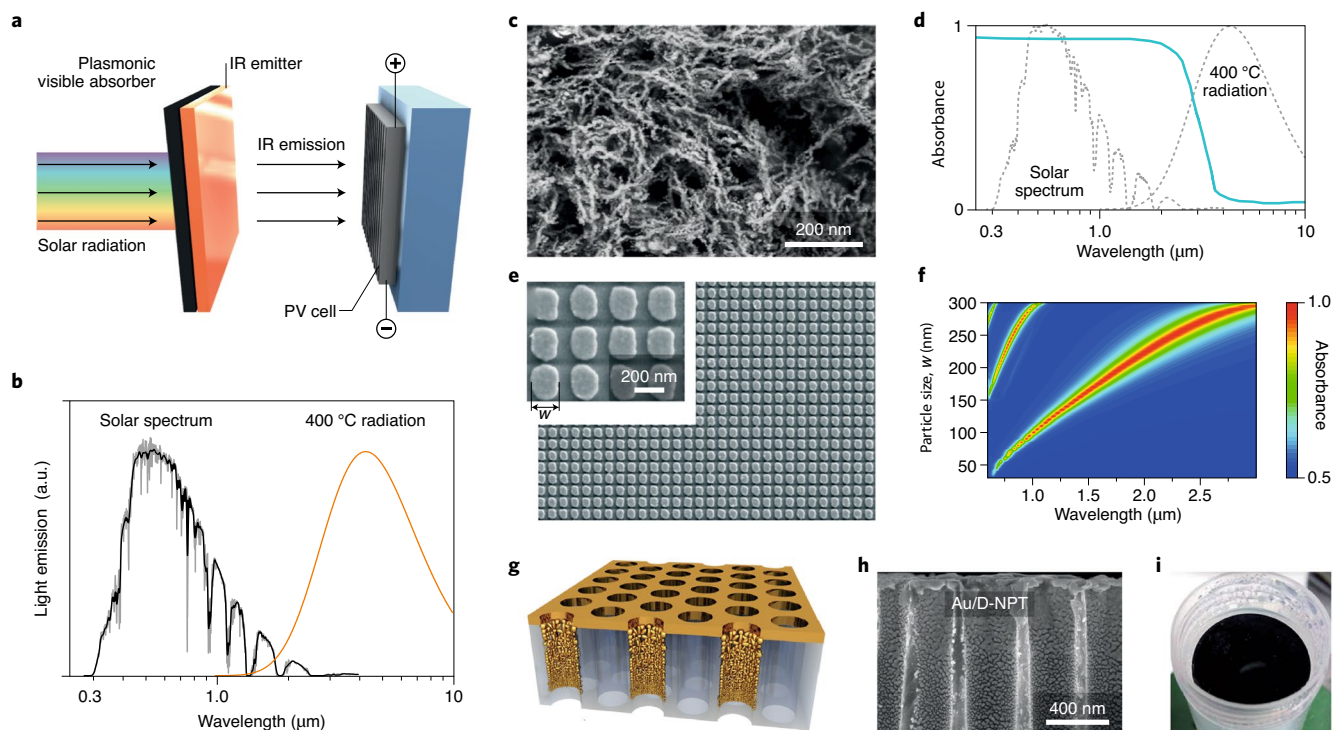


**Fig. 3 | Thermoplasmonics for solar-light harvesting.** **a**, Sketch of principle of a plasmonic-assisted thermophotovoltaic (PV) cell. **b**, Solar spectra irradiance and 400 °C blackbody spectral radiance, per unit wavelength (arbitrary units). **c**, SEM image of nickel nanochains. **d**, Absorbance spectrum of a Ni nanochain solution, compared with the solar spectrum and the black body spectrum at 400 °C (grey dashed lines) depicted in **b**. **e, f**, SEM image of gold nanopads of size  $w$  deposited on an Au- $\text{Al}_2\text{O}_3$  substrate (**e**), along with the absorbance spectra as a function of  $w$  (**f**). **g–i**, Self-assembled aluminium porous structure decorated with gold nanoparticles (Au/D-NPT) for broadband absorption (**g**), associated SEM image (**h**) and photograph of the Au/D-NPT solution (**i**). Panels adapted with permission from: **c, d**, ref. <sup>67</sup>, AIP; **e, f**, ref. <sup>70</sup>, AIP; **g–i**, ref. <sup>89</sup>, AAAS.

processes involves the heating of seawater with subsequent condensation<sup>84</sup>. Solar-thermal desalination requires first of all absorber materials with a high efficiency of converting the harvested solar photons into heat. Two materials are commonly considered — carbonaceous materials and plasmonic materials. Carbon-based materials such as carbon black, graphite, graphene or other forms of graphitic materials are often used as broadband absorber materials relying on the  $\pi$ -electron absorption (Box 2) with absorptivity of 80% to almost 100% over a wide range from the ultraviolet to the NIR (up to 2.5  $\mu\text{m}$  wavelength)<sup>87,88</sup>. Plasmonic materials have recently gained attention as an efficient absorber material with efficient light-to-heat conversion, but is not always cheap<sup>89,90</sup>. To cover the whole spectral range of solar illumination, plasmonic materials require a size dispersion or more complex geometries, such as particle aggregates or porous structures. Absorptivities of 95% and higher have been reached with gold, silver or aluminium-based materials (Fig. 3g–i)<sup>89–91</sup>. Using such absorbers, solar steam generation and desalination has been demonstrated. Researchers have recently reported a self-assembled aluminium nanoparticle-based porous system for an effective desalination<sup>90</sup>. Others have decorated natural wood with plasmonic metals to create high solar conversion efficiencies for steam generation<sup>91</sup>. Yet, the biggest issue for solar-thermal desalination is not primarily related to the efficient light-to-heat conversion but rather to the thermal management. Desalination by evaporation requires a supply of the latent heat of evaporation of water. This energy is almost three orders of magnitude higher than the free energy of mixing<sup>84,86</sup>. Without a recovery of the latent heat during the condensation process, the energy requirement would be two to three orders of magnitude higher than the reverse osmosis processes. Even with an efficient latent heat

recovery, a specific energy consumption of about 40  $\text{kW h m}^{-3}$  is required, which is still considerably above reverse osmosis processes driven by photovoltaic electricity<sup>86</sup>. Thus, the future application of solar-thermal desalination, including approaches based on efficient plasmonic absorbers, seems to be limited to areas of hypersaline solutions with large salinity where high water recovery is required<sup>84</sup>. Here, again, as for all applications based on solar absorption, the interest in plasmonic nanoparticles over black absorbers made of dyes or carbon black is not obvious, as discussed in Box 2.

### Soft matter and fluids

Many experiments in plasmonics involve a liquid medium, the dynamics of which is highly temperature dependent. Temperature variations in liquids can yield a rich variety of processes, such as enhanced Brownian motion, thermo-viscous effects, convection, phase transition (such as bubble formation, polymer melting, sintering and so on), thermo-osmosis and thermophoresis. This section is devoted to explaining the interest in studying soft matter in thermoplasmonics with a special focus on four effects: thermally induced flows, thermophoresis, bubble formation and powder sintering for additive manufacturing, the latter being a rare example of industrial application of thermoplasmonics.

**Temperature-induced liquid flows.** Temperature gradients in fluids can generate fluid convection for which the overheated parts are moving upward. The magnitude of this effect depends on the temperature increase, the size of the heat source and the confinement of the fluid along the vertical direction. Convection of liquids induced by optically heated plasmonic nanostructures on a substrate has been studied numerically as a function of the liquid film thickness<sup>92</sup>.

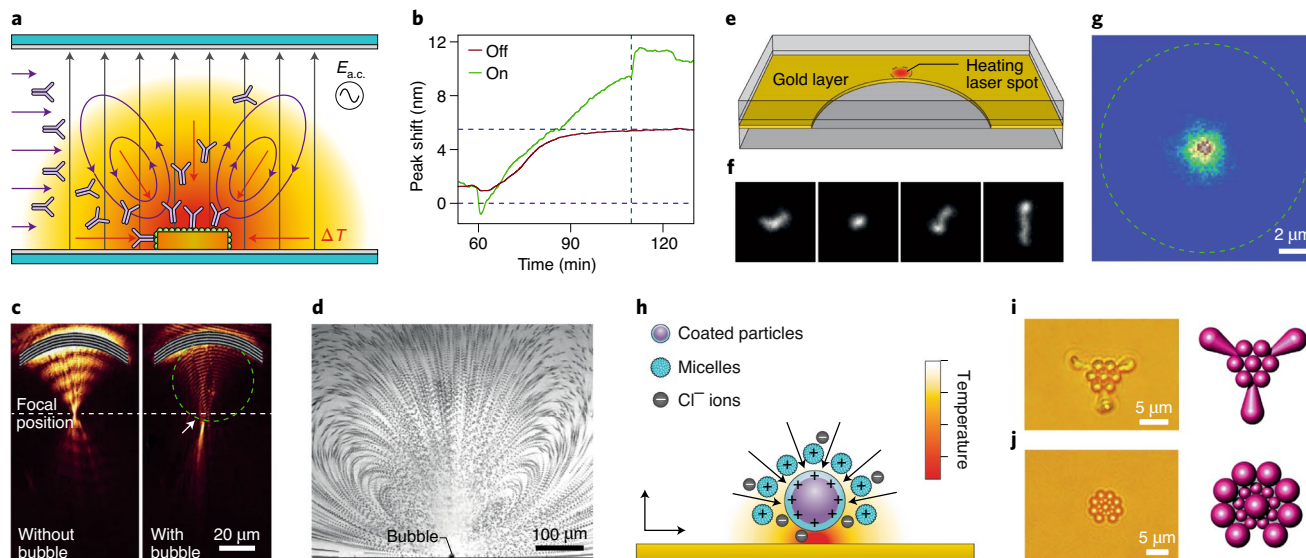


**Fig. 4 | Thermoplasmonics in liquids.** **a**, Electrothermoplasmonic sensors, which efficiently transport target molecules (Y-shaped) to plasmonic sensing structures (gold disk) by a combination of thermal (colour gradient) and a.c. electric fields ( $E_{a.c.}$ ; arrows). **b**, The plasmonic resonance shift of the sensor for different operation modes, with (green) and without (brown) using the electrothermoplasmonic effect. **c**, Reconfigurable plasmo-fluidic lens. A laser-induced bubble modifies the surface plasmon propagation in a thin gold film. **d**, Marangoni flows around a bubble generated by an optically heated gold nanoisland film in water. **e**, Thermophoretic trapping of single  $\lambda$ -DNA molecules in dynamic temperature fields generated by focusing a laser on the rim of a hole in a thin gold film. **f, g**, Snapshots of the  $\lambda$ -DNA at different times (**f**) and the position statistics (blue to red colour map) in the trap (**g**). The trap edge is indicated by the dashed line. **h**, Opto-thermoelectric tweezers based on a thermoplasmonic heating of a nanoplasmonic substrate and a thermo-electric charge separation. **i, j**, Optothermal assembly of colloidal superstructures based on thermal-induced depletion forces using non-spherical and spherical (**i**) as well as spherical particles of different size (**j**), as observed in bright field microscopy. Panels adapted with permission from: **a, b**, ref.<sup>94</sup>, American Chemical Society; **c**, ref.<sup>123</sup>, Springer Nature Ltd; **d**, ref.<sup>113</sup>, Springer Nature Ltd; **e–g**, ref.<sup>105</sup>, American Chemical Society; **h–j**, ref.<sup>106</sup>, AAAS.

For liquid heights of above 100  $\mu\text{m}$ , several hundred nanometres per second flow velocity has been predicted, while in more confined microfluidic channels (<10  $\mu\text{m}$  high) convection is negligible. Yet, convective flows in such settings can be boosted by combining temperature-induced electrical conductivity changes with a.c. electric fields<sup>93</sup>. This approach, called electro-thermoplasmonics, has been exploited to load plasmonic traps as well as to overcome the diffusion limit in localized surface plasmon resonance biosensing (Fig. 4a,b)<sup>94</sup>. Temperature gradients above heated metal films also lead to changes in the local viscosity. Moving the heating spot on the surface generates a thermo-viscous motion of particles in the travelling viscosity gradient that can be used without plasmonic structures to generate flows in living cells<sup>95</sup>. Besides that, the generation of temperature gradients by plasmonic nanoparticles along solid/liquid boundaries also naturally leads to thermo-osmotic flows<sup>96</sup> with speeds easily reaching 100  $\mu\text{m s}^{-1}$  being strongly confined to the interfacial region and the driving source of thermophoresis.

**Microscale thermophoresis.** Thermophoresis, also known as the Ludwig–Soret effect, denotes the migration of solutes (colloids, molecules) in fluids due to the existence of temperature gradients, while the fluid is at rest<sup>97,98</sup>. The magnitude of this effect for a given solute, usually occurring from hot to cold regions, is given by the thermophoretic mobility  $D_T$ , linking the solutes thermophoretic velocity  $v$  and the temperature gradient such that  $v = -D_T \nabla T$  (ref.<sup>98</sup>). The strength of this effect compared with the solution diffusion coefficient  $D$  can be better judged using the Soret coefficient  $S_T = D_T/D$ . The mechanisms of thermophoresis are well understood in gases and in most liquids except for water. In liquids, thermophoresis is driven by thermo-osmotic flows arising from the perturbation of the liquid–solid interfacial interactions by the temperature gradients<sup>96</sup>.

Thermophoretic effects have been studied for decades, usually with infrared lasers to heat the solvent directly<sup>99,100</sup> or other absorbing structures<sup>101</sup>, and applied as a tool to study binding kinetics in ensembles of proteins by just using the fact that proteins change their thermophoretic mobility upon binding<sup>102</sup>.

A chromium-coated surface as an absorbing medium was first used to generate microscale temperature gradients and to manipulate colloids<sup>103</sup> with a reduced laser power down to 1 mW. The opaque metal layer, however, precludes the use of optical microscope studies in transmission. They also yield weaker temperature gradients. Herein lies the benefit of plasmonic nanoparticles (Box 3). In 2013, it was proposed to apply thermoplasmonics to microscale thermophoresis experiments. Static and dynamic temperature fields generated by controlled heating of plasmonic gold nanostructures at a surface allowed researchers to trap single 200 nm polymer colloids in solution<sup>104</sup>. In 2015, the trapping of even single or a well-defined number of multiple  $\lambda$ -DNA molecules in water with the help of temperature fields generated by a feedback algorithm<sup>105</sup> was achieved (Fig. 4e–g).

Other work presented a platform that is based on thermally generated electric fields (Fig. 4h–j)<sup>106</sup>. Surfactant molecules with dissociated counterions migrate with different mobilities in the temperature gradient to set up a thermoelectric field to move other objects. By using this effect with a nanoplasmonic substrate (essentially a dense nanoparticle film), the authors could trap gold nanoparticles of different shapes, colloids, vesicles or cells<sup>107</sup>. While not all of the effects in these experiments are understood, they demonstrate the power of using thermophoresis as a tool for material science and analytics. These demonstrations are now at a point where thermophoresis with plasmonic structures is turned into a tool, for example, to study the aggregation of proteins, which is of foremost interest in the study of neurodegenerative diseases<sup>34</sup>.

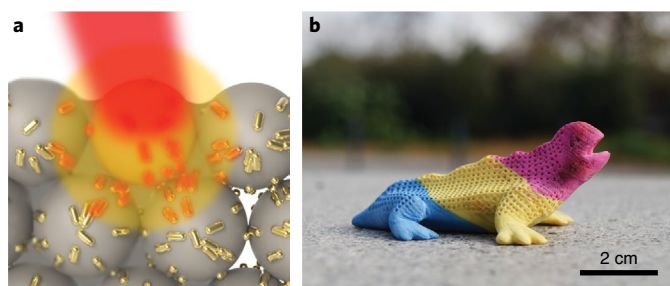


**Fig. 5 | Thermoplasmonics in manufacturing.** **a**, Artistic illustration of the sintering of adjacent polymer beads induced by light-to-heat conversion in gold nanorods. **b**, Example of a colourful sintered object printed with a PA12 powder using an invisible gold nanorod ink combined with standard dyes. Figure adapted with permission from ref. <sup>129</sup>, American Chemical Society.

Even if there is still some way to go to reach the goal of predicting thermophoretic effects from the fundamental interfacial properties, its importance for microfluidic analytical processes, the design of active matter<sup>108</sup> and the transport of molecules in systems involving plasmon assisted chemistry and catalysis will become exponentially important in the near future.

**Microbubble formation.** When heating plasmonic nanoparticles in a liquid, a bubble is bound to appear above a certain light power. This effect has been studied in detail for two decades under nano- to femtosecond-pulsed illumination<sup>109,110</sup> for applications in biomedicine, such as cancer therapy, photoacoustic imaging or optoporation. The interest in continuous-wave illumination is much more recent. When one or several plasmonic nanoparticles are distributed on a substrate and illuminated in a liquid, above a certain light power, a bubble can nucleate at the interface<sup>111</sup>. This ‘surface bubble’ (SB) usually remains attached (at least in the case of water) to the liquid/solid interface, featuring a truncated spherical shape. The beauty of this system is the rich and unexpected physics: in water, an SB forms around 200 °C (not at 100 °C)<sup>31</sup>, it is stable for several seconds to several minutes at ambient temperature<sup>31,112</sup>, it yields dramatic convection in the surrounding liquid<sup>113</sup> (Fig. 4d) and it can be moved on the substrate at high speed by moving the heating laser. All these singular phenomena led to original fundamental articles and some practical applications. For instance, an SB provides an interesting tool in the context of optofluidics<sup>114,115</sup>, for microscale manipulation of beads<sup>116,117</sup>, biomolecules<sup>118</sup>, ions<sup>119</sup> and liquids<sup>120,121</sup>; and also for the manipulation of light, such as for light modulation<sup>122</sup> or focusing<sup>123</sup> (Fig. 4c). Many studies have been devoted to the understanding of the underlying physics of SBs<sup>124</sup>, and of the associated effects. In this field of research, the use of plasmonic nanoparticles is not always justified or necessary (Box 2). As a matter of fact, many studies of SBs have been performed on metal layers or on indium tin oxide. One can expect many other studies in this field as the behaviour of SBs (temperature onset, fluid convection, dynamics, life time and so on) strongly depends on the surrounding fluid. Experiments in alcohols and alkanes have already been reported very recently<sup>125,126</sup>.

**Additive manufacturing.** Another field that can greatly benefit from thermoplasmonics is three-dimensional printing, also known as additive manufacturing. Three-dimensional printing has quickly developed over the past decade and is becoming the preferred production approach for many objects of our everyday life. There exist many three-dimensional printing approaches, each having pros and cons. One of them relies on powder sintering<sup>127</sup>, which consists of scanning a high-power CO<sub>2</sub> laser to directly heat up polymer

particles to sintering. To overcome the use of a bulky and expensive infrared laser, it was proposed to use photothermal sensitizers, in particular, carbon black, combined with cheap and compact visible/NIR laser sources<sup>128</sup>. The main issue of using carbon black though is the resulting dark grey–black colour of the print (Box 2), which is incompatible with colourful final objects (or at least would require extensive post-processing).

Thermoplasmonics offers an appealing way around carbon black limitations. By designing an invisible ink, made of plasmonic nanoparticles resonant in the NIR of the spectrum, one can achieve white prints, offering the possibility to add standard dyes to achieve colourful prints (Fig. 5)<sup>129</sup>. Albeit promising, the use of plasmonics in additive manufacturing raises several important questions. Plasmonic metals have non-zero absorption in the visible range (interband transitions and/or transverse mode in the case of nanorods), which limits how white the print can be. When projecting market applications, there is also an issue related to production cost of the ink. For both reasons, there is a need to find some alternative materials.

## Outlook

Thermoplasmonics turned into an asset what has long been considered as a major drawback of plasmonics, namely metal losses. Atypically, this Review tackles concepts related to many fields of science at once, namely cell biology, chemistry, medicine, material science, optics, thermodynamics, fluid dynamics, nanooptics, solar energy harvesting and more. This diversity stems from the ubiquity of thermal-induced effects in all fields of science. Such richness is the fingerprint of thermoplasmonics, which has, over the past two decades, become a driving force to create synergies between different scientific disciplines. For these reasons, we foresee that thermoplasmonics will remain a blossoming field of research for decades, where the only limitation in the development of other applications will be the imagination.

Received: 27 January 2020; Accepted: 8 June 2020;  
Published online: 17 August 2020

## References

- Hüttmann, G. & Birngruber, R. On the possibility of high-precision photothermal microeffects and the measurement of fast thermal denaturation of proteins. *IEEE J. Sel. Top. Quantum Electron.* **5**, 954–962 (1999).
- Boyer, D., Tamarat, P., Maali, A., Lounis, B. & Orrit, M. Photothermal imaging of nanometer-sized metal particles among scatterers. *Science* **297**, 1160–1163 (2002).
- Pitsillides, C. M., Joe, E. K., Wei, X., Anderson, R. R. & Lin, C. P. Selective cell targeting with light-absorbing microparticles and nanoparticles. *Biophys. J.* **84**, 4023–4032 (2003).
- Hirsch, L. R. et al. Nanoshell-mediated near-infrared thermal therapy of tumors under magnetic resonance guidance. *Proc. Natl Acad. Sci. USA* **100**, 13549–13554 (2003).
- Ghosh, P., Han, G., De, M., Kim, C. K. & Rotello, V. M. Gold nanoparticles in delivery applications. *Adv. Drug Deliv. Rev.* **60**, 1307–1315 (2008).
- Li, W. & Chen, X. Gold nanoparticles for photoacoustic imaging. *Nanomedicine* **10**, 299–320 (2015).
- Baffou, G. & Quidant, R. Thermo-plasmonics: using metallic nanostructures as nano-sources of heat. *Laser Photon. Rev.* **7**, 171–187 (2013).
- Baffou, G. *Thermoplasmonics* (Cambridge Univ. Press, 2017).
- Jauffred, L., Samadi, A., Klingberg, H., Bendix, P. M. & Oddershede, L. B. Plasmonic heating of nanostructures. *Chem. Rev.* **119**, 8087–8130 (2019).
- Govorov, A. O. & Richardson, H. H. Generating heat with metal nanoparticles. *Nano Today* **2**, 30–38 (2007).
- Wilhelm, S. et al. Analysis of nanoparticle delivery to tumours. *Nat. Rev. Mater.* **1**, 16014 (2016).
- Morales-Dalmau, J., Vilches, C., De Miguel, I., Sanz, V. & Quidant, R. Optimum morphology of gold nanorods for light-induced hyperthermia. *Nanoscale* **10**, 2632–2638 (2018).
- Pilot study of AuroLase(tm) therapy in refractory and/or recurrent tumors of the head and neck. ClinicalTrials NCT00848042 *ClinicalTrials.gov* <https://clinicaltrials.gov/ct2/show/NCT00848042> (2017).

14. Ali, M. R. K., Ibrahim, I. M., Ali, H. R., Selim, S. A. & El-Sayed, M. A. Treatment of natural mammary gland tumors in canines and felines using gold nanorods-assisted plasmonic photothermal therapy to induce tumor apoptosis. *Int. J. Nanomed.* **11**, 4849–4863 (2016).
15. Feliu, N. et al. In vivo degeneration and the fate of inorganic nanoparticles. *Chem. Soc. Rev.* **45**, 2440–2457 (2016).
16. Nichols, J. W. & Bae, Y. H. EPR: Evidence and fallacy. *J. Control. Release* **190**, 451–464 (2014).
17. Poon, W. et al. Elimination pathways of nanoparticles. *ACS Nano* **13**, 5785–5798 (2019).
18. Morales-Dalmau, J. et al. Quantification of gold nanoparticle accumulation in tissue by two-photon luminescence microscopy. *Nanoscale* **11**, 11331–11339 (2019).
19. Beik, J. et al. Gold nanoparticles in combinatorial cancer therapy strategies. *Coord. Chem. Rev.* **387**, 299–324 (2019).
20. Krpetić, Ž. et al. Inflicting controlled nonthermal damage to subcellular structures by laser-activated gold nanoparticles. *Nano Lett.* **10**, 4549–4554 (2010).
21. Vankayala, R., Huang, Y. K., Kalluru, P., Chiang, C. S. & Hwang, K. C. First demonstration of gold nanorods-mediated photodynamic therapeutic destruction of tumors via near infra-red light activation. *Small* **10**, 1612–1622 (2014).
22. Kharlamov, A. N. et al. Silica-gold nanoparticles for atheroprotective management of plaques: results of the NANOM-FIM trial. *Nanoscale* **7**, 8003–8015 (2015).
23. Wilson, A. M. et al. In vivo laser-mediated retinal ganglion cell optoporation using KV1.1 conjugated gold nanoparticles. *Nano Lett.* **18**, 6981–6988 (2018).
24. Harris, T. & Kim, A. Hair removal with coated metal nanoparticles. US patent 14/471,331 (2014).
25. Paithankar, D. Y. et al. Acne treatment based on selective photothermolysis of sebaceous follicles with topically delivered gold plasmonic particles. *Adv. Mater. TechConnect Briefs* **2016** **3**, 177–179 (2016).
26. Zharov, V. P., Mercer, K. E., Galitovskaya, E. N. & Smeltzer, M. S. Photothermal nanotherapeutics and nanodiagnostics for selective killing of bacteria targeted with gold nanoparticles. *Biophys. J.* **90**, 619–627 (2006).
27. Pihl, M., Bruzell, E. & Andersson, M. Bacterial biofilm elimination using gold nanorod localised surface plasmon resonance generated heat. *Mater. Sci. Eng. C* **80**, 54–58 (2017).
28. De Miguel, I. et al. Plasmon-based biofilm inhibition on surgical implants. *Nano Lett.* **19**, 2524–2529 (2019).
29. Neumann, O. et al. Compact solar autoclave based on steam generation using broadband light-harvesting nanoparticles. *Proc. Natl Acad. Sci. USA* **110**, 11677–11681 (2013).
30. Robert, H. M. L. et al. Photothermal control of heat-shock protein expression at the single cell level. *Small* **14**, 42–47 (2018).
31. Baffou, G., Polleux, J., Rigneault, H. & Monneret, S. Super-heating and micro-bubble generation around plasmonic nanoparticles under cw illumination. *J. Phys. Chem. C* **118**, 4890–4898 (2014).
32. Kyrsting, A., Bendix, P. M., Stamou, D. G. & Oddershede, L. B. Heat profiling of three-dimensionally optically trapped gold nanoparticles using vesicle cargo release. *Nano Lett.* **11**, 888–892 (2011).
33. Hrelescu, C. et al. DNA melting in gold nanostove clusters. *J. Phys. Chem. C* **114**, 7401–7411 (2010).
34. Fränzl, M. et al. Thermophoretic trap for single amyloid fibril and protein aggregation studies. *Nat. Methods* **16**, 611–614 (2019).
35. Zhu, M., Baffou, G., Meyerbröker, N. & Polleux, J. Micropatterning thermoplasmonic gold nanoarrays to manipulate cell adhesion. *ACS Nano* **6**, 7227–7233 (2012).
36. Baumgart, J. et al. Off-resonance plasmonic enhanced femtosecond laser optoporation and transfection of cancer cells. *Biomaterials* **33**, 2345–2350 (2012).
37. Li, M., Lohmüller, T. & Feldmann, J. Optical injection of gold nanoparticles into living cells. *Nano Lett.* **15**, 770–775 (2015).
38. Bahadori, A., Oddershede, L. B. & Bendix, P. M. Hot-nanoparticle-mediated fusion of selected cells. *Nano Res.* **10**, 2034–2045 (2017).
39. Boulais, E., Lachaine, R., Hatfe, A. & Meunier, M. Plasmonics for pulsed-laser cell nanosurgery: fundamentals and applications. *J. Photochem. Photobiol. C* **17**, 26–49 (2013).
40. Parakhonskiy, B. V., Parak, W. J., Volodkin, D. & Skirtach, A. G. Hybrids of polymeric capsules, lipids, and nanoparticles: thermodynamics and temperature rise at the nanoscale and emerging applications. *Langmuir* **35**, 8574–8583 (2019).
41. Ambrosone, A. et al. Control of Wnt/ $\beta$ -catenin signaling pathway in vivo via light responsive capsules. *ACS Nano* **10**, 4828–4834 (2016).
42. Carregal-Romero, S. et al. NIR-light triggered delivery of macromolecules into the cytosol. *J. Control. Release* **159**, 120–127 (2012).
43. Giner-Casares, J. J., Henriksen-Lacey, M., García, I. & Liz-Marzán, L. M. Plasmonic surfaces for cell growth and retrieval triggered by near-infrared light. *Angew. Chem. Int. Ed.* **55**, 974–978 (2016).
44. Baffou, G. & Quidant, R. Nanoplasmonics for chemistry. *Chem. Soc. Rev.* **43**, 3898–3907 (2014).
45. Shin, H. H., Koo, J. J., Lee, K. S. & Kim, Z. H. Chemical reactions driven by plasmon-induced hot carriers. *Appl. Mater. Today* **16**, 112–119 (2019).
46. Qiu, J. & Wei, W. D. Surface plasmon-mediated photothermal chemistry. *J. Phys. Chem. C* **118**, 20735–20749 (2014).
47. Cao, L., Barsic, D. N., Guichard, A. R. & Brongersma, M. L. Plasmon-assisted local temperature control to pattern individual semiconductor nanowires and carbon nanotubes. *Nano Lett.* **7**, 3523–3527 (2007).
48. Baffou, G. & Rigneault, H. Femtosecond-pulsed optical heating of gold nanoparticles. *Phys. Rev. B* **84**, 1–13 (2011).
49. Haruta, M., Kobayashi, T., Sano, H. & Yamada, N. Novel gold catalysts for the oxidation of carbon monoxide at a temperature far below 0 °C. *Chem. Lett.* **16**, 405–408 (1987).
50. Boyd, D. A., Greengard, L., Brongersma, M., Ei-Naggar, M. Y. & Goodwin, D. G. Plasmon-assisted chemical vapor deposition. *Nano Lett.* **6**, 2592–2597 (2006).
51. Chen, X., Zhu, H. Y., Zhao, J. C., Zheng, Z. F. & Gao, X. P. Visible-light-driven oxidation of organic contaminants in air with gold nanoparticle catalysts on oxide supports. *Angew. Chem. Int. Ed.* **47**, 5353–5356 (2008).
52. Hung, W. H., Aykol, M., Valley, D., Hou, W. & Cronin, S. B. Plasmon resonant enhancement of carbon monoxide catalysis. *Nano Lett.* **10**, 1314–1318 (2010).
53. Adleman, J. R., Boyd, D. A., Goodwin, D. G. & Psaltis, D. Heterogenous catalysis mediated by plasmon heating. *Nano Lett.* **9**, 4417–4423 (2009).
54. Fasciani, C., Alejo, C. J. B., Grenier, M., Netto-Ferreira, J. C. & Scaiano, J. C. High-temperature organic reactions at room temperature using plasmon excitation: decomposition of dicumyl peroxide. *Org. Lett.* **13**, 204–207 (2011).
55. Robert, H. M. L. et al. Light-assisted solvothermal chemistry using plasmonic nanoparticles. *ACS Omega* **1**, 2–8 (2016).
56. Tian, Y. & Tatsuma, T. Plasmon-induced photoelectrochemistry at metal nanoparticles supported on nanoporous TiO<sub>2</sub>. *Chem. Commun.* **16**, 1810–1811 (2004).
57. Christopher, P., Xin, H. & Linic, S. Visible-light-enhanced catalytic oxidation reactions on plasmonic silver nanostructures. *Nat. Chem.* **3**, 467–472 (2011).
58. Ingram, D. B. & Linic, S. Water splitting on composite plasmonic-metal/semiconductor photoelectrodes: evidence for selective plasmon-induced formation of charge carriers near the semiconductor surface. *J. Am. Chem. Soc.* **133**, 5202–5205 (2011).
59. Dubi, Y., Un, I. W. & Sivan, Y. Thermal effects — an alternative mechanism for plasmon-assisted photocatalysis. *Chem. Sci.* **11**, 5017–5027 (2020).
60. Baffou, G., Bordacchini, I., Baldi, A. & Quidant, R. Simple experimental procedures to distinguish photothermal from hot-carrier processes in plasmonics. *Light. Sci. Appl.* **9**, 108 (2020).
61. Shockley, W. & Queisser, H. J. Detailed balance limit of efficiency of p–n junction solar cells. *J. Appl. Phys.* **32**, 510–519 (1961).
62. Dimroth, F. et al. Four-junction wafer-bonded concentrator solar cells. *IEEE J. Photovolt.* **6**, 343–349 (2016).
63. Zhou, Z., Sakr, E., Sun, Y. & Bermel, P. Solar thermophotovoltaics: reshaping the solar spectrum. *Nanophotonics* **5**, 1–21 (2016).
64. Omair, Z. et al. Ultraefficient thermophotovoltaic power conversion by band-edge spectral filtering. *Proc. Natl Acad. Sci. USA* **116**, 15356–15361 (2019).
65. Albrecht, G., Kaiser, S., Giessen, H. & Hentschel, M. Refractory plasmonics without refractory materials. *Nano Lett.* **17**, 6402–6408 (2017).
66. Chester, D., Bermel, P., Joannopoulos, J. D., Soljacic, M. & Celanovic, I. Design and global optimization of high-efficiency solar thermal systems with tungsten cermet. *Opt. Express* **19**, A245–A257 (2011).
67. Wang, X., Li, H., Yu, X., Shi, X. & Liu, J. High-performance solution-processed plasmonic Ni nanochain-Al<sub>2</sub>O<sub>3</sub> selective solar thermal absorbers. *Appl. Phys. Lett.* **101**, 203109 (2012).
68. Guler, U., Boltasseva, A. & Shalae, V. M. Refractory plasmonics. *Science* **344**, 263–264 (2014).
69. Arpin, K. A. et al. Three-dimensional self-assembled photonic crystals with high temperature stability for thermal emission modification. *Nat. Commun.* **4**, 2630 (2013).
70. Hao, J. et al. High performance optical absorber based on a plasmonic metamaterial. *Appl. Phys. Lett.* **96**, 251104 (2010).
71. Li, W. et al. Plasmonics: refractory plasmonics with titanium nitride: broadband metamaterial absorber. *Adv. Mater.* **26**, 7921–7921 (2014).
72. Chirumamilla, M. et al. Metamaterial emitter for thermophotovoltaics stable up to 1400 °C. *Sci. Rep.* **9**, 7241 (2019).
73. Laroche, M., Carminati, R. & Greffet, J.-J. Near-field thermophotovoltaic energy conversion. *J. Appl. Phys.* **100**, 063704 (2006).
74. Ilic, O., Jablan, M., Joannopoulos, J. D., Celanovic, I. & Soljacic, M. Overcoming the black body limit in plasmonic and graphene near-field thermophotovoltaic systems. *Opt. Express* **20**, A366–A384 (2012).

75. Guo, Y., Molesky, S., Hu, H., Cortes, C. L. & Jacob, Z. Thermal excitation of plasmons for near-field thermophotovoltaics. *Appl. Phys. Lett.* **105**, 073903 (2014).
76. Messina, R. & Ben-Abdallah, P. Graphene-based photovoltaic cells for near-field thermal energy conversion. *Sci. Rep.* **3**, 1383 (2013).
77. Fiorino, A. et al. Nanogap near-field thermophotovoltaics. *Nat. Nanotechnol.* **13**, 806–811 (2018).
78. Angayarkanni, S. A. & Philip, J. Review on thermal properties of nanofluids: recent developments. *Adv. Colloid Interface Sci.* **225**, 146–176 (2015).
79. Liu, X. & Xuan, Y. Full-spectrum volumetric solar thermal conversion: via photonic nanofluids. *Nanoscale* **9**, 14854–14860 (2017).
80. Ni, G. et al. Volumetric solar heating of nanofluids for direct vapor generation. *Nano Energy* **17**, 290–301 (2015).
81. Ishii, S., Sugavaneshwar, R. P. & Nagao, T. Titanium nitride nanoparticles as plasmonic solar heat transducers. *J. Phys. Chem. C* **120**, 2343–2348 (2016).
82. Chen, M., He, Y., Zhu, J. & Kim, D. R. Enhancement of photo-thermal conversion using gold nanofluids with different particle sizes. *Energy Convers. Manag.* **112**, 21–30 (2016).
83. Rativa, D. & Gómez-Malagón, L. A. Solar radiation absorption of nanofluids containing metallic nanoellipsoids. *Sol. Energy* **118**, 419–425 (2015).
84. Wang, Z. et al. Pathways and challenges for efficient solar-thermal desalination. *Sci. Adv.* **5**, eaax076 (2019).
85. Elimelech, M. & Phillip, W. A. The future of seawater desalination: energy, technology, and the environment. *Science* **333**, 712–717 (2011).
86. Al-Karaghoul, A. & Kazmerski, L. L. Energy consumption and water production cost of conventional and renewable-energy-powered desalination processes. *Renew. Sustain. Energy Rev.* **24**, 343–356 (2013).
87. Ito, Y. et al. Multifunctional porous graphene for high-efficiency steam generation by heat localization. *Adv. Mater.* **27**, 4302–4307 (2015).
88. Liu, Y., Chen, J., Guo, D., Cao, M. & Jiang, L. Floatable, self-cleaning, and carbon-black-based superhydrophobic gauze for the solar evaporation enhancement at the air–water interface. *ACS Appl. Mater. Interfaces* **7**, 13645–13652 (2015).
89. Zhou, L. et al. Self-assembly of highly efficient, broadband plasmonic absorbers for solar steam generation. *Sci. Adv.* **2**, e1501227 (2016).
90. Zhou, L. et al. 3D self-assembly of aluminium nanoparticles for plasmon-enhanced solar desalination. *Nat. Photon.* **10**, 393–398 (2016).
91. Zhu, M. et al. Plasmonic wood for high-efficiency solar steam generation. *Adv. Energy Mater.* **8**, 1701028 (2018).
92. Donner, J. S., Baffou, G., McCloskey, D. & Quidant, R. Plasmon-assisted optofluidics. *ACS Nano* **5**, 5457–5462 (2011).
93. Ndukaife, J. C. et al. Long-range and rapid transport of individual nano-objects by a hybrid electrothermoplasmonic nanotweezer. *Nat. Nanotechnol.* **11**, 53–59 (2016).
94. Garcia-Guirado, J. et al. Overcoming diffusion-limited biosensing by electrothermoplasmonics. *ACS Photon.* **5**, 3673–3679 (2018).
95. Mittasch, M. et al. Non-invasive perturbations of intracellular flow reveal physical principles of cell organization. *Nat. Cell Biol.* **20**, 344–351 (2018).
96. Bregulla, A. P., Würger, A., Günther, K., Mertig, M. & Cichos, F. Thermo-osmotic flow in thin films. *Phys. Rev. Lett.* **116**, 188303 (2016).
97. Würger, A. Thermal non-equilibrium transport in colloids. *Rep. Prog. Phys.* **73**, 126601 (2010).
98. Piazza, R. Thermophoresis: moving particles with thermal gradients. *Soft Matter* **4**, 1740–1744 (2008).
99. Duhr, S., Arduini, S. & Braun, D. Thermophoresis of DNA determined by microfluidic fluorescence. *Eur. Phys. J. E* **15**, 277–286 (2004).
100. Maeda, Y. T., Buguin, A. & Libchaber, A. Thermal separation: interplay between the Soret effect and entropic force gradient. *Phys. Rev. Lett.* **107**, 38301 (2011).
101. Thamdrup, L. H., Larsen, N. B. & Kristensen, A. Light-induced local heating for thermophoretic manipulation of DNA in polymer micro- and nanochannels. *Nano Lett.* **10**, 826–832 (2010).
102. Wienken, C. J., Baaske, P., Rothbauer, U., Braun, D. & Duhr, S. Protein-binding assays in biological liquids using microscale thermophoresis. *Nat. Commun.* **1**, 100 (2010).
103. Jiang, H. R., Wada, H., Yoshinaga, N. & Sano, M. Manipulation of colloids by a nonequilibrium depletion force in a temperature gradient. *Phys. Rev. Lett.* **102**, 100–103 (2009).
104. Braun, M. & Cichos, F. Optically controlled thermophoretic trapping of single nano-objects. *ACS Nano* **7**, 11200–11208 (2013).
105. Braun, M., Bregulla, A. P., Günther, K., Mertig, M. & Cichos, F. Single molecules trapped by dynamic inhomogeneous temperature fields. *Nano Lett.* **15**, 5499–5505 (2015).
106. Lin, L. et al. Opto-thermophoretic assembly of colloidal matter. *Sci. Adv.* **3**, e1700458 (2017).
107. Lin, L., Peng, X. & Zheng, Y. Reconfigurable opto-thermoelectric printing of colloidal particles. *Chem. Commun.* **53**, 7357–7360 (2017).
108. Khadka, U., Holubec, V., Yang, H. & Cichos, F. Active particles bound by information flows. *Nat. Commun.* **9**, 3864 (2018).
109. Metwally, K., Mensah, S. & Baffou, G. Fluence threshold for photothermal bubble generation using plasmonic nanoparticles. *J. Phys. Chem. C* **119**, 28586–28596 (2015).
110. Lombard, J., Biben, T. & Merabia, S. Threshold for vapor nanobubble generation around plasmonic nanoparticles. *J. Phys. Chem. C* **121**, 15402–15415 (2017).
111. Xie, Y. & Zhao, C. An optothermally generated surface bubble and its applications. *Nanoscale* **9**, 6622–6631 (2017).
112. Kim, N., Park, H. & Do, H. Evolution of cavitation bubble in tap water by continuous-wave laser focused on a metallic surface. *Langmuir* **35**, 3308–3318 (2019).
113. Namura, K., Nakajima, K. & Suzuki, M. Quasi-stokeslet induced by thermoplasmonic Marangoni effect around a water vapor microbubble. *Sci. Rep.* **7**, 45776 (2017).
114. Chen, J. et al. Thermal optofluidics: principles and applications. *Adv. Opt. Mater.* **8**, 1900829 (2020).
115. Wang, M. et al. Plasmo-fluidics: merging light and fluids at the micro-/nanoscale. *Small* **11**, 4423–4444 (2015).
116. Lin, L. et al. Bubble-pen lithography. *Nano Lett.* **16**, 701–708 (2016).
117. Zhao, C. et al. Theory and experiment on particle trapping and manipulation via optothermally generated bubbles. *Lab Chip* **14**, 384–391 (2014).
118. Yamamoto, Y. et al. Macroscopically anisotropic structures produced by light-induced solvothermal assembly of porphyrin dimers. *Sci. Rep.* **8**, 11108 (2018).
119. Li, Y. et al. Photoresistance switching of plasmonic nanopores. *Nano Lett.* **15**, 776–782 (2015).
120. Namura, K. et al. Direction control of quasi-stokeslet induced by thermoplasmonic heating of a water vapor microbubble. *Sci. Rep.* **9**, 4770 (2019).
121. Zhang, K. et al. Laser-induced thermal bubbles for microfluidic applications. *Lab Chip* **11**, 1389 (2011).
122. Heber, A., Selmke, M. & Cichos, F. Metal nanoparticle based all-optical photothermal light modulator. *ACS Nano* **8**, 1893–1898 (2014).
123. Zhao, C., Liu, Y., Zhao, Y., Fang, N. & Huang, T. J. A reconfigurable plasmo-fluidic lens. *Nat. Commun.* **4**, 2305 (2013).
124. Lombard, J., Biben, T. & Merabia, S. Nanobubbles around plasmonic nanoparticles: thermodynamic analysis. *Phys. Rev. E* **91**, 43007 (2015).
125. Jollans, T. & Orrit, M. Explosive, oscillatory, and Leidenfrost boiling at the nanoscale. *Phys. Rev. E* **99**, 63110 (2019).
126. Zaytsev, M. E. et al. Plasmonic bubbles in *n*-alkanes. *J. Phys. Chem. C* **122**, 28375–28381 (2018).
127. Simonot, A., Cassaignau, A. & Coré-Bailtais, M. *The State of 3D Printing* (Sculpteo, 2015); [https://www.sculpteo.com/media/ebook/State\\_of\\_3DP\\_2018.pdf](https://www.sculpteo.com/media/ebook/State_of_3DP_2018.pdf)
128. Wagner, T., Höfer, T., Knies, S. & Eyerer, P. Laser sintering of high temperature resistant polymers with carbon black additives. *Int. Polym. Process.* **19**, 395–401 (2004).
129. Powell, A. W., Stavrinadis, A., De Miguel, I., Konstantatos, G. & Quidant, R. White and brightly colored 3D printing based on resonant photothermal sensitizers. *Nano Lett.* **18**, 6660–6664 (2018).
130. Lalisie, A., Tessier, G., Plain, J. & Baffou, G. Quantifying the efficiency of plasmonic materials for near-field enhancement and photothermal conversion. *J. Phys. Chem. C* **119**, 25518–25528 (2015).
131. Baffou, G., Quidant, R. & Girard, C. Heat generation in plasmonic nanostructures: influence of morphology. *Appl. Phys. Lett.* **94**, 153109 (2009).
132. Wang, X., Santschi, C. & Martin, O. J. F. Strong improvement of long-term chemical and thermal stability of plasmonic silver nanoantennas and films. *Small* **13**, 1700044 (2017).
133. MacKey, M. A., Ali, M. R. K., Austin, L. A., Near, R. D. & El-Sayed, M. A. The most effective gold nanorod size for plasmonic photothermal therapy: theory and in vitro experiments. *J. Phys. Chem. B* **118**, 1319–1326 (2014).
134. Park, S. E. et al. Comparative hyperthermia effects of silica-gold nanoshells with different surface coverage of gold clusters on epithelial tumor cells. *Int. J. Nanomed.* **10**, 261–271 (2015).
135. Chen, J. et al. Immuno gold nanocages with tailored optical properties for targeted photothermal destruction of cancer cells. *Nano Lett.* **7**, 1318–1322 (2007).
136. Chatterjee, H., Rahman, D. S., Sengupta, M. & Ghosh, S. K. Gold nanostars in plasmonic photothermal therapy: the role of tip heads in the thermoplasmonic landscape. *J. Phys. Chem. C* **122**, 13082–13094 (2018).
137. Quintanilla, M. et al. Heat generation by branched Au/Pd nanocrystals: influence of morphology and composition. *Nanoscale* **11**, 19561–19570 (2019).
138. Baffou, G., Quidant, R. & García De Abajo, F. J. Nanoscale control of optical heating in complex plasmonic systems. *ACS Nano* **4**, 709–716 (2010).

139. Baffou, G. et al. Photoinduced heating of nanoparticle arrays. *ACS Nano* **7**, 6478–6488 (2013).
140. Richardson, H. H., Carlson, M. T., Tandler, P. J., Hernandez, P. & Govorov, A. O. Experimental and theoretical studies of light-to-heat conversion and collective heating effects in metal nanoparticle solutions. *Nano Lett.* **9**, 1139–1146 (2009).

### Acknowledgements

We acknowledge financial support from the European Research Council programme under grants ERC-CoG QnanoMECA (64790) and ERC-CoG HiPhore (772725), Fundació Privada Cellex, the CERCA programme, the Spanish Ministry of Economy and Competitiveness, through the ‘Severo Ochoa’ Programme for Centres of Excellence in R&D (SEV-2015-0522), the Deutsche Forschungsgemeinschaft (DFG, project numbers 237143019, 336492136, 203317744), the

ESF and the Free State of Saxony (Junior Research Group UniDyn, project number SAB 100382164).

### Competing interests

The authors declare no competing interests.

### Additional information

**Correspondence** should be addressed to G.B., F.C. or R.Q.

**Reprints and permissions information** is available at [www.nature.com/reprints](http://www.nature.com/reprints).

**Publisher's note** Springer Nature remains neutral with regard to jurisdictional claims in published maps and institutional affiliations.

© Springer Nature Limited 2020